ARTICLE

JAAS
www.rsc.org/jaas

Laser-induced breakdown spectroscopy of liquid droplets: correlation analysis with plasma-induced current *versus* continuum background

Jer-Shing Huang and King-Chuen Lin*

Department of Chemistry, National Taiwan University, Taipei 106 and Institute of Atomic and Molecular Sciences, Academia Sinica, Taipei 106 Taiwan. E-mail: kclin@ccms.ntu.edu.tw; Fax: 886-2-23621483

Received 30th July 2004, Accepted 9th November 2004
First published as an Advance Article on the web 9th December 2004

We have developed a current normalization method for laser-induced breakdown spectroscopy (LIBS) for analyzing liquid droplets. An electrospray ionization device is employed to generate a stream of microdroplets. The spray needle serves as the anode, through which the analyte solution is spread toward the other metal base which is the cathode. Upon laser irradiation at the liquid droplets, the time-resolved laser-induced breakdown (LIB) emission and plasma-induced current signals are acquired concurrently on a single-shot basis. The plot of LIB emission intensity against the current intensity yields a straight line. The slopes in the correlation plots increase with the sample concentration, whereby the calibration curve is obtained. The resultant limit of detection (LOD) of Na sample may reach 0.6 ± 0.1 mg l^{-1}, about 20 times better than that obtained by LIB/background normalization. The impinging laser energy dependence of both normalization methods is also investigated. The correlation linearity for the background normalization is found to be restricted within a small range of laser energy. When a two-line ratio is involved to account for the plasma temperature, its linear feature is markedly improved. According to the Boltzmann equation, the plasma temperature as a function of delay time relative to the onset of continuum background is determined to gain insight into the temperature effect on the LIB/background method. In contrast, the LIB/current method, which has taken into account the ablated amount of microdroplets and the plasma excitation temperature, retains correlation linearity over a much wider range of laser energy.

I. Introduction

As an emerging analytical technique for rapid material analysis applied in industry and environmental science, laser-induced breakdown spectroscopy (LIBS) is advantageous because of its capabilities of multi-elemental detection, minimal sample preparation, non-invasive analysis and suitability for remote measurement.[1–9] Nevertheless, it suffers from severe emission signal fluctuation, which is caused by sources such as laser pulse fluctuation, sample inhomogeneity, and the inverse bremsstrahlung radiation.[1,10–13]

To compensate for this signal fluctuation, the average method over a number of laser shots is usually used, but the improvement of the signal-to-noise (S/N) ratio is offset by the nonlinear optical ablation effect.[14,15] Internal standard method is an alternative solution *via* the measurement of the intensity ratio of analyte and reference element.[16–19] The application of internal standardization to the chemical analysis of the multi-component samples requires knowledge of the internal standard concentrations. The reference element should also be assumed to have the same fluctuation pattern as that of the analyzed sample.[15,19,20] To overcome this problem, Winefordner and co-workers developed a calibration approach based on the linear regression coefficient calculated between spectra of a range of certified standards and the spectrum of a reference sample.[21] Without using any normalization, this method was demonstrated in the analysis of binary alloys using LIBS to give rise to results accurate to approximately 5% for major components. Schechter and co-workers adopted a correlation plot of analyte signal *versus* background to determine the sample concentration.[15] They measured a sequence of spectra from single breakdown events in detecting trace metals in soil and aerosols. The line peak of analyte was found to correlate well with the baseline, which had the same multiplicative fluctuation as the sample signal. This method does not depend on a constant constituent of a reference element involved.

As with the method of internal standardization, external reference normalization is similarly reported to be useful in reducing the laser-induced breakdown (LIB) signal fluctuation. For instance, Cheung and Young, by applying LIBS in a liquid jet, found that the single-shot LIB signal with the corresponding acoustic normalization showed a linear relationship with the impinging pulse energy.[14] The slope obtained by the plot of normalized LIB emission *versus* pulse energy may yield information of the sample concentration. Chaleard *et al*. quantized the LIB emission signals in air at atmospheric pressure by taking intensities of the emission lines as a function of the vaporized mass and the plasma excitation temperature.[22] The ablated mass was accounted for by using an acoustic signal and excitation temperature was measured by a two-line method. Normalization of the LIB emission signals by these two parameters allowed for an accurate determination of Cu and Mn in various alloy matrices. Hakkanen *et al*. analyzed inhomogeneous paper coatings and found linear correlations between the LIB emission signals and the coat weight and the binder contents of the coatings.[23]

Applications of LIBS in liquid state are sparse compared with those in solid state. In recent years, we have developed a correlation method based on plasma-induced current normalization for analysis of the sample droplets.[24] Instead of using bulk or jet as the liquid sampling methods,[6,14,15] we have used an electrospray ionization needle to generate microdroplets of metal salt solutions in the study of matrix effects on the LIBS.[25] The LIB and plasma-induced current signals were detected simultaneously on a single-shot basis.[24] We found that the intensities of single-shot time-resolved LIB emission may linearly correlate with the corresponding current intensities.

DOI: 10.1039/b411719k

Given the calibration curve obtained from the slopes of the correlation plots, the limit of detection (LOD) for the Na analysis may reach 1 mg l^{-1}, even with the matrix salts add up to 2000 mg l^{-1}.[25] The current normalization method is capable of suppressing the signal fluctuation, improving the LOD determination and concurrently correcting the matrix effect. Although LIBS applied in liquid state cannot be more sensitive than the conventional detection methods such as flame emission or furnace absorption, it resists matrix interference without losing much sensitivity. LIBS may also be operated in a hostile environment, which becomes difficult for conventional optical methods. In this work, we take a step further to characterize both normalization methods of LIB/current and LIB/background as a function of the laser energy and compare the resultant LOD of Na sample solution. We also discuss in detail the factor of plasma temperature, which should play an important role especially in the LIB/background normalization.

II. Experimental

A. LIBS setup

Laser source. A schematic diagram for the LIBS system is illustrated in Fig. 1. In brief, a third harmonic Nd : YAG laser (DCR-2A, Spectra-Physics), operated at 10 Hz with duration of 5–8 ns, emitting at 355 nm, was used as the light source. The incident pulse was focused through a 10-cm focal length quartz lens onto the microdroplets generated by an electrospray ionization needle. The pulse energy prior to the quartz lens was controlled in the range 9–45 mJ, which was monitored constantly with an energy meter. The pulse-to-pulse fluctuation remained at ±5%.

Microdroplet generation and data acquisition. A home-made electrospray ionization device was employed to generate a stream of microdroplets, as described previously.[24,25] The analyte solution was syringe-pumped into a 200-μm id stainless steel spray needle. The needle was biased at 3 kV as the anode, through which the analyte solution was sprayed toward the other metal base as the cathode. The analyte solution broke into droplets as carrier solvent evaporated.[26–28] The laser pulse interacted with the sprayed droplets ~2 mm downstream from the needle tip. The irradiated spot was close to the tip of Taylor cone where a higher density of microdroplets could be gained.[29,30] The luminous plume produced was imaged with a set of 15 and 20 cm focal length lenses onto a 0.35 m Czerny–Turner monochromator (Model 270, McPherson,) behind which a photomultiplier tube (PMT, R955, Hamamatsu) was mounted. To avoid the influence of plume instability caused by variation of the irradiated spot size from shot to shot, the slits were opened to 500 μm wide, allowing transmission of the total plasma plume. A theoretical spectral resolution of 1 nm is obtained for the monochromator with a reciprocal dispersion of 20 Å mm^{-1}. Meanwhile, the slit width was narrow enough to substantially reduce the transmitted continuum background at the specific wavelength of LIB emission.

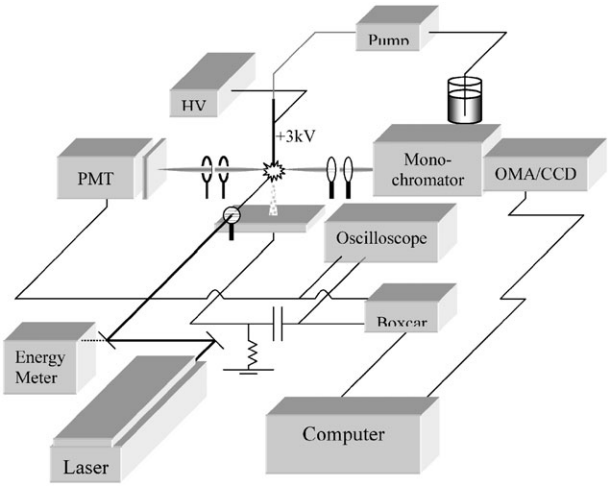

Fig. 1 Schematic diagram of LIBS setup.

The time-resolved LIB emission obtained was fed into either a transient digitizer (Model 9450A, LeCroy) for single-shot profile recording or a boxcar integrator (Model SR250, Stanford Research System) for signal processing. The time-resolved spectra of the analyte were integrated within a gate, which was opened at 900 ns delay relative to the onset of the continuum background emission. The LIB emission could then be the least interfered with by the intense continuum background. The gate width was optimized to 12 μs. The adjustment of the gate width and position may help suppress the LIB signal fluctuation to improve the signal-to-noise ratio.

Reagents. The Na and Ca elements as the analyte were made from their chloride solutions. A 1000 mg l^{-1} chloride (Reagent grade, Merck) solution was first prepared with water–methanol (1 : 1 v/v) (HPLC grade, Baker) as solvent and then diluted to the desired concentrations. For gaining a better electrospray efficiency, we used a water–methanol (1 : 1 v/v) mixed solvent throughout this work.

B. Detection of current and background emission

The current was collected from the cathode *via* a high-pass filter into a second channel of either a transient digitizer or a boxcar integrator. It was monitored concurrently with the LIB emission. The current profile oscillated rapidly on a ns scale, as indicated in the previous work.[24,25] Its first maximum peak was then integrated within a 20 ns gate throughout all the experiments. A better LIB/current correlation linearity must rely on an appropriate adjustment of the current gate width and position. For instance, when the gate width remained the same, but the position was slightly shifted by <5 ns away from the onset of the current profile, the regression coefficient downgraded by 7%.[25] In fact, an appropriate selection of RC time constant may slow down the oscillation and prolong the life time of each peak.

Meanwhile, the correlation between the LIB signal and the continuum background was also analyzed from the same time-resolved spectrum. The background emission was integrated immediately following its onset within a 100 ns gate, while the LIB emission signal was integrated within a 12 μs gate in 900 ns delay. Although the plasma composition including continuum background, molecular emission, and atomic emission is hardly temporally isolated, the behavior of continuum background emission can be traced by substitution of the blank solution.[24] Its maximum emission lasts for hundreds of ns and then decays rapidly close to the baseline. The gate width and position for the sample LIB signal are so selected as to gain the maximum intensity of LIB emission, but minimum interference from the continuum background.

C. Plasma temperature measurement

The LIB spectra in frequency domain of the Ca sample used for the measurement of plasma temperature were detected with a CCD (512 × 512, DV412 BV, Andor Technology) mounted behind a monochromator. The read mode of CCD with temperature controlled at −60 °C was set at single track so that it functioned as a diode array for spectrum acquisition. The Ca^{+} ion emissions at six different wavelengths in the range from 310 to 400 nm were detected in either 0 or 900 ns delay relative to the background emission, with each line acquired for 2000 shots to improve the signal-to-noise ratio.

The background contribution evaluated at near off-resonance has been subtracted; the instrument response, including grating transmittance efficiency and CCD quantum efficiency, has been taken into account to correct the data of the Ca^+ emissions at different wavelengths. A Boltzmann equation is applied to determine the plasma temperature based on the multiple line intensities.

For the experiment of plasma temperature correction, a two-line ratio was adopted, comprising two emission lines of Ca^+ ion in the $4p^2P_{1/2,3/2} \rightarrow 4s^2S_{1/2}$ transitions at 396.85 and 393.37 nm, respectively. These two lines were detected with an optical multichannel analyzer (OMA) (OMA III, Model 1460, EG&G PARC) mounted behind a monochromator centered at 395 nm. The OMA detector with temperature at −20 °C was triggered by a pulse generator (Model 1304, EG&G PARC), acquiring the spectral data through a scan control card (Model 1463, EG&G PARC).

III. Results and discussion

A. Limit of detection between LIB/current and LIB/background

As with our previous work,[24,25] a stream of single-shot time-dependent LIB emission spectra can be acquired upon laser irradiation of the sample microdroplets. The temporal profile begins with an intense peak which contributes to the continuum background and decays by several tens to hundreds of ns, independent of the wavelengths selected. Then LIB emission rises markedly in hundreds of ns delay. The intensity of LIB emission integrated from the profile can be linearly correlated with the plasma-induced current intensity. As is shown in Fig. 2, a plot of the Na LIB emission intensity against the current intensity yields a straight line, of which the slope increases as the concentrations of the analyte solution increase. The obtained regression coefficients for the slopes are larger than 0.95.

As was mentioned under Introduction, the continuum background emission in the frequency domain has been widely adopted to correlate with the LIB emission to diminish the shot-to-shot signal fluctuation. The continuum emission originates from a complicated superposition of various continuum spectra including the radiation from free-free transition, recombination of free electron and ion, free-bound transition and pseudo-continuum of strongly broadened lines.[6,31] Similar to the analysis used in the frequency domain,[15] in this work the signal intensities of LIB and background emission may be obtained from the integration of a time-resolved profile within an individual gate. Fig. 3 shows a linear plot of the LIB emission against the background emission on a single-shot basis, yielding a slope sensitive to the concentration variation.

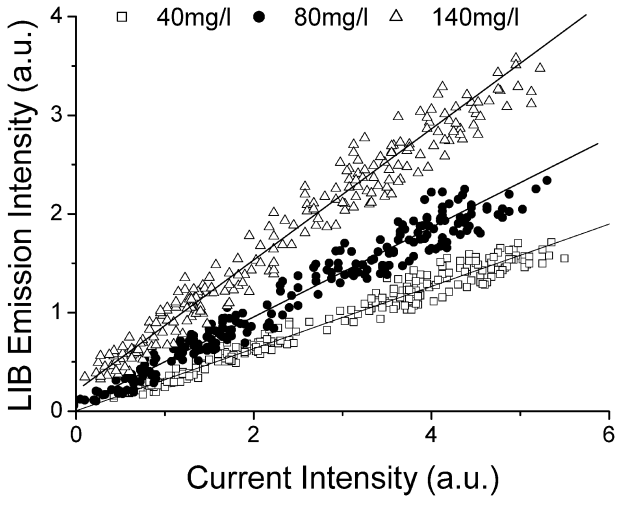

Fig. 2 Shot-to-shot correlation plot of LIB emission *versus* plasma-induced current as a function of Na concentration. The regression coefficients are 0.982, 0.980 and 0.984 for the concentration 140, 80 and 40 mg l^{-1}, respectively.

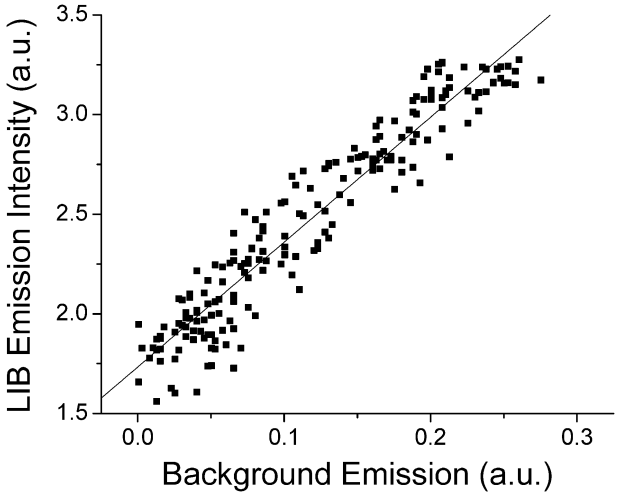

Fig. 3 Shot-to-shot correlation plot (with regression coefficient 0.953) of Na LIB emission *versus* continuum background emission at laser energy 21 mJ.

The slopes obtained in either LIB/current or LIB/background plots as a function of the sample concentration give rise to a calibration curve, as shown in Fig. 4. Note that the calibration curves do not pass through the origin. This is caused by the fact that the slope of the correlation plot for the blank solution is not zero.[24] It suggests that the LIBS signal and continuum background emission may not be completely temporally demarcated. Since the same magnitude of background is contributed to all other measurements for different concentrations of sample, the small, non-zero background does not affect the determination of sensitivity of the calibration curve. In the case of current normalization, given the standard deviation of the blank solution, σ, obtained from the slope of the correlation plot and the slope of the calibration curve, m, the limit of detection (LOD), as defined by $2\sigma/m$, reaches 0.6 ± 0.1 mg l^{-1} for the Na sample at a pulse energy 23 mJ. The LOD and the linear dynamic range have been substantially improved in comparison with the treatment by averaging spectral intensities over the same number of laser pulses.[24] In contrast, for the case of background normalization, the sensitivity obtained by the calibration curve along with the standard deviation of the blank solution may result in a LOD of 11.6 mg l^{-1} for the

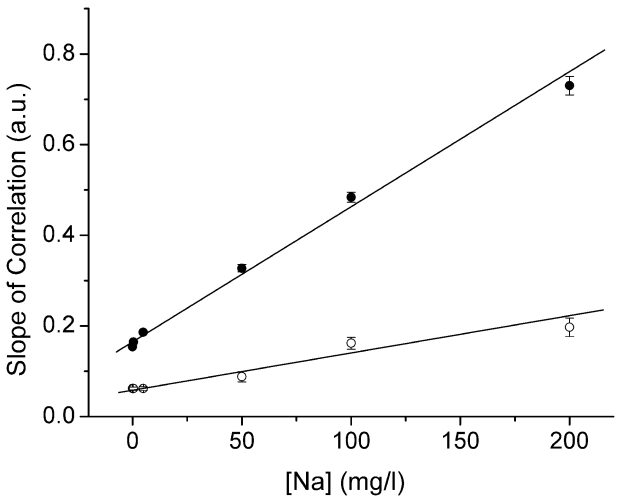

Fig. 4 Calibration curves for the Na concentration obtained with the correlation methods of LIB/current (●) and LIB/background (○), respectively. The laser energy is at 23 mJ.

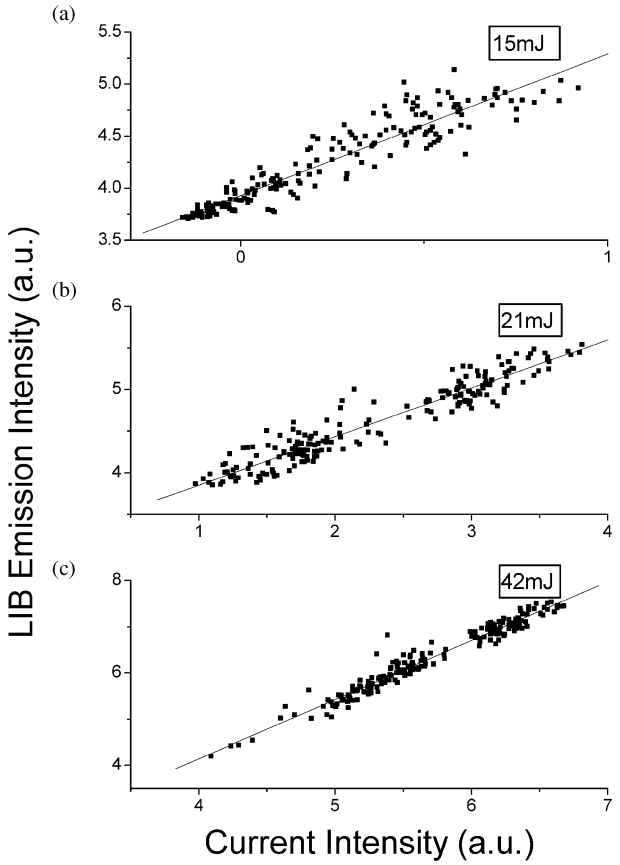

Fig. 5 Correlation plots of LIB emission of Na sample at 200 mg l^{-1} *versus* current intensity obtained at the laser energy of (a) 15 (regression coefficient $R = 0.942$), (b) 21($R = 0.954$) and (c) 42 mJ ($R = 0.977$).

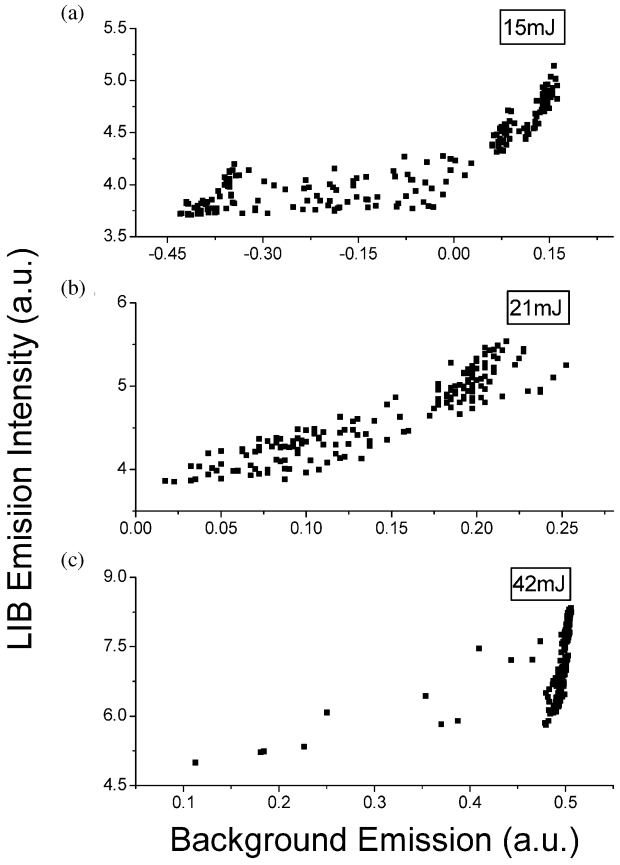

Fig. 6 Correlation plots of LIB emission of Na sample at 200 mg l^{-1} *versus* continuum background emission obtained at the laser energy of (a) 15, (b) 21 and (c) 42 mJ.

Na sample at the same laser energy 23 mJ, which is about 20 times worse than that determined in the LIB/current correlation method. The standard deviation of the blank solution determined in the background normalization method is five to six times larger than that with the current normalization. The gate width and position over the background emission have been varied and turn out to have similar results.

B. Laser energy dependence

In addition to the LOD comparison, we characterize the laser energy dependence of these two correlation methods. As shown in Fig. 5, when the laser energy at 355 nm is controlled in the range of 9–45 mJ, the correlation between the LIB and the current intensities remains a straight line whereby the calibration curve may be obtained. As reported, the resulting LOD of Na sample may be improved by increasing the laser energy.[24] The linear relationship found between the LIB and current signals implies that the emission signal results substantially from the breakdown event rather than the laser-induced excitation/emission, with which the plasma-induced current may otherwise exhibit random correlation. Since the generation of microdroplets facilitates sample vaporization, atomization and excitation/ionization efficiency, lower laser energies than in most LIBS experiments can thus be adopted to cause the breakdown emission.

In contrast, the linearity for the Na LIB/background correlation holds only within a small range of laser energy about 21 mJ in this experiment. As shown in Fig. 6, when the energy is reduced to 15 mJ, the LIB emission signal begins to rise almost exponentially with the background emission. At reduced laser energy, the background emission signal is sensitive to the energy fluctuation, while the LIB emission rises only when the energy exceeds a threshold. Our work shows that the correlation linearity may not hold unless the threshold energy of air breakdown is reached. Nevertheless, the background emission can be easily saturated as the energy is larger than 25 mJ (Fig. 6).

C. Plasma temperature correction for continuum background emission

The nonlinear response for the LIB/background correlation in the low laser energy region might be caused by the lack of plasma temperature consideration. As reported by Winefordner and co-workers in observing the laser ablation of alloy, the LIB emission and background emission can be linearly correlated only when the electron temperature retains constant in the plasma plume.[19] In studying LIB emissions of Pb and Ba contained in the sand and soil samples, Eppler *et al.* related the influence on the LIB measurement to plasma excitation conditions, physical properties of the sample compound, matrix absorptivity, electron density and plasma temperature.[32] The plasma temperature apparently plays an important role which needs to be considered in the standardization of LIB emission.

To verify this point, we adopt a two-line ratio method to monitor the plasma temperature. The Na sample is changed to Ca for a better selection of the two emission lines. In this case, the Ca^+ ion emitting at 396.8 and 393.4 nm for the $4p^2P_{1/2} \rightarrow 4s^2S_{1/2}$ and $4p^2P_{3/2} \rightarrow 4s^2S_{1/2}$ transitions, respectively, are detected. As depicted in Fig. 1, an additional OMA detector is employed to acquire these two emission lines, while the other PMT is used to detect the time-resolved LIB emission of Ca atom in the $4s4p^1P \rightarrow 4s^2\ ^1S$ transition at 422.7 nm. The obtained background emission is first normalized to an area ratio of the two emission lines acquired without any time delay on a single-shot basis. Then the LIB intensity is plotted against the normalized background intensity, as in the case of the Na

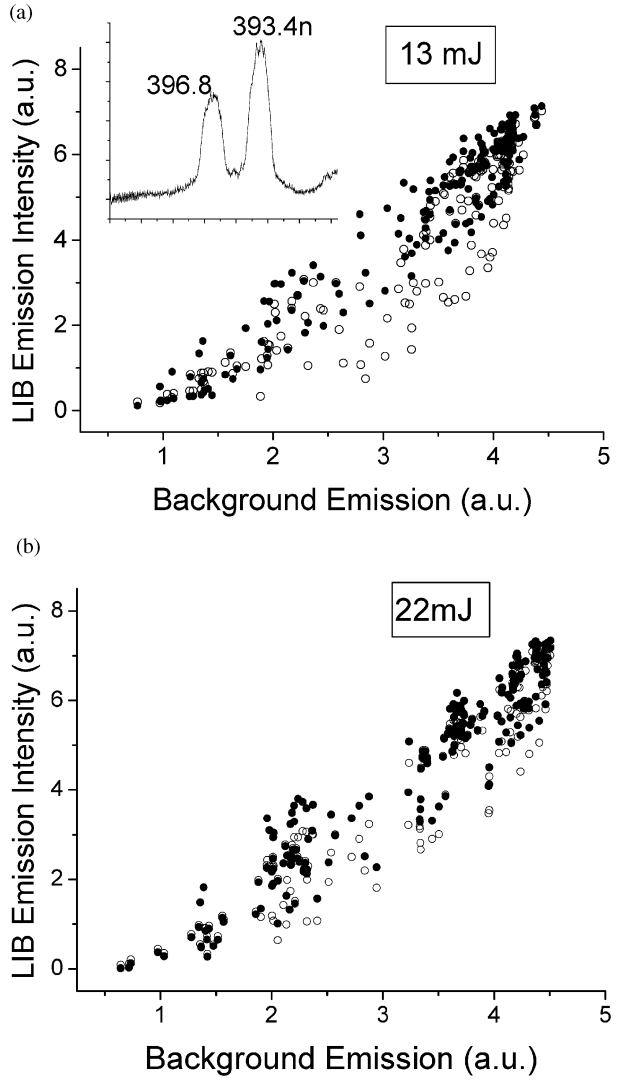

Fig. 7 Correlation plot of LIB emission of Ca *versus* continuum background emission obtained at the laser energies of (a) 13 mJ and (b) 22 mJ. (○) Denotes the background emission without plasma temperature correction. (●) Denotes the background emission normalized by an area ratio of two emission lines, which are acquired without any time delay relative to the background emission. These two emission spectra acquired by an OMA detector are displayed in the inset.

sample. After correction for the plasma temperature, Fig. 7(a) shows that deviation from linearity in the Ca LIB/background plot observed at low energy, 13 mJ, has been markedly reduced. When the energy is increased to 22 mJ, the LIB/background correlation may hold a straight line without any correction, as mentioned in the preceding section. At this energy, the linear feature remains almost the same before and after the temperature correction, as shown in Fig. 7(b). The accuracy of the two-line method depends on the energy difference of the upper states with respect to kT (k is Boltzmann constant) and the related oscillator strength.[33] In spite of small energy difference, 222 cm^{-1}, between the upper states, the selected two-line ratio of Ca^+ fine-structure doublets seems appropriate to serve as a temperature correction factor. For cooler plasma conditions, like this work with low breakdown energy, the shot-to-shot variation of two-line ratio may reflect sensitively the fluctuation of background emission due to the temperature factor.

In the above treatment, we simply correct the factor of background plasma temperature. If the temperature gradient is non-zero, the continuum background and LIB signals, which are acquired in 0 and 900 ns delay, respectively, should both

Table 1 Multiple emission lines of Ca^+ ion used in determination of plasma temperature

λ/nm	E_k/cm^{-1}	g_k	Transition	$A_{ki}/(10^8)$ s^{-1}
315.886	56 839.25	4	$4d^2D_{3/2} \rightarrow 4p^2P_{1/2}$	3.1
317.933	56 858.46	6	$4d^2D_{5/2} \rightarrow 4p^2P_{3/2}$	3.6
370.602	52 166.93	2	$5s^2S_{1/2} \rightarrow 4p^2P_{1/2}$	0.88
373.690	52 166.93	2	$5s^2S_{1/2} \rightarrow 4p^2P_{3/2}$	1.7
393.366	25 414.40	4	$4p^2P_{3/2} \rightarrow 4s^2S_{1/2}$	1.47
396.846	25 191.51	2	$4p^2P_{1/2} \rightarrow 4s^2S_{1/2}$	1.4

take into account the plasma temperature to improve the correlation linearity. Why can linearity of LIB/background be improved significantly even though the LIB signal is not corrected with the factor of plasma temperature? To answer this question, one should know how the plasma temperature changes in time delay of 0 and 900 ns relative to the onset of continuum background emission. Thus, we take a step further to determine temperature of the plasma plume at the times to acquire background and LIB signals by using multiple-line ratios based on the Boltzmann equation. According to the equation which assumes existence of local thermal equilibrium in the plasma plume, the intensity of a spectral line I_{ki} emitting from the upper level k to the lower level i may be expressed as[6,33]

$$I_{ki} = q\left(\frac{1}{\lambda}\right)(g_k)(A_{ki})\exp\left(\frac{-E_k}{k_b T}\right) \qquad (1)$$

where q denotes the instrument and optical alignment factor, λ is the emitting wavelength, g_k the statistical weight for the upper level k, A_{ki} the Einstein emission coefficient from the k to i level, k_b the Boltzmann constant, E_k the upper level energy and T the plasma temperature. When q is fixed, the Boltzmann plot of In ($I_{ki}\lambda/g_kA_{ki}$) *versus* E_k yields a slope indicative of the plasma temperature. The multiple-line ratios, which take into account several pairs of energy difference between the upper states, turn out to be more appropriate than the two-line method to quantify the plasma temperature.

For the Ca case, as listed in Table 1, six transition lines selected in the Boltzmann plot comprise three pairs of fine-structure doublets as the upper states emitting in the range 315–400 nm. The emission lines obtained at the laser energy 28 mJ are fitted with Lorentzian function to resolve the spectral overlap of the fine-structure doublets and then integrated to obtain individual line intensity I_{ki}. As is shown in Fig. 8, the slope obtained in the Boltzmann plot yields temperature of

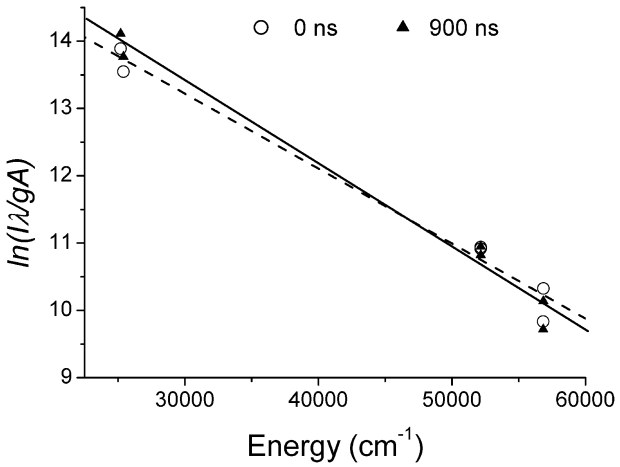

Fig. 8 Boltzmann plot of Ln($I\lambda/gA$) *versus* the upper state energy (see text for the notation). The Ca^+ ion spectra of multiple emission lines are acquired in 0 (○, —) ns and 900 (▲, —) ns delay, respectively, relative to the continuum background emission.

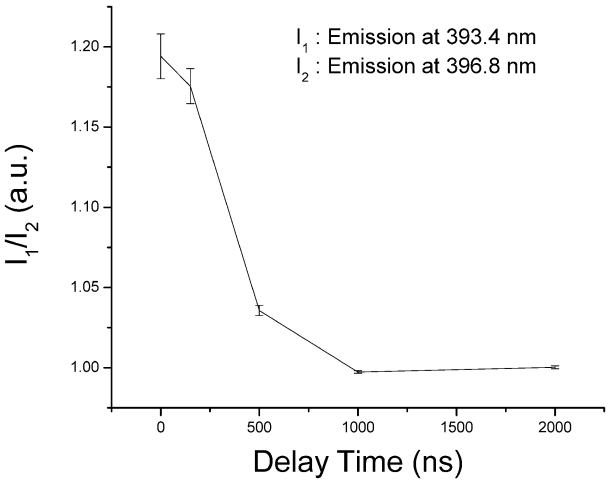

Fig. 9 Two-line ratios obtained from Ca^+ ion emission at 393.4 and 396.8 nm as a function of delay time relative to the onset of background emission.

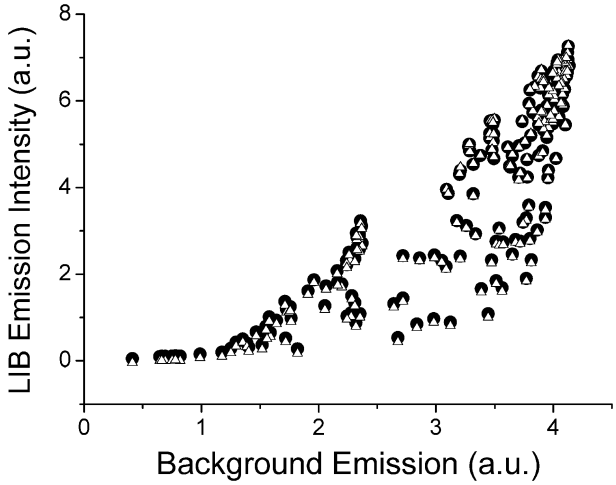

Fig. 10 Correlation plot of LIB emission of Ca *versus* continuum background emission obtained at a laser energy of 13 mJ. (●) Denotes the background emission without plasma temperature correction. (△) Denotes the background emission normalized by an area ratio of two emission lines, which are acquired in 900 ns delay relative to the background emission.

12 900 ± 900 and 11 700 ± 700 K for a delay of 0 and 900 ns, respectively. The temperature turns cool by about 1200 ± 1100 K. Note that the plasma temperature behaves differently from that detected in metal aerosols by Yalcin *et al.* with pulse energy of 40–150 mJ at 532 nm.[34] At least two aspects may explain the difference. First, a much smaller breakdown energy at 28 mJ was used in this work such that a lower temperature may result in the plasma. Second, a sampling method with microdroplet generation was adopted, different from the way used to form the metal aerosols. Thus, it is not surprising to find different temperature-cooling behavior. While the uncertainty range is considered, the temperature decay difference becomes smaller.

The temperature change at these two delay times can alternatively be monitored by measuring the two-line ratios. The two emission lines acquired at different delay times are averaged over 2000 laser shots. Fig. 9 shows the time delay dependence of the area ratio of the two emission lines from the fine-structure doublets of the Ca^+ ion in the $4p^2P_{1/2,3/2} \rightarrow 4s^2S_{1/2}$ transitions at 396.85 and 393.37 nm, respectively. The decrease tendency of the ratio reflects the temperature decrease with the time delay. One should note that the temperature fluctuation is markedly reduced with increase in the time delay. Since the standard deviation of the ratio at the time to acquire the LIB signal is relatively small, one can realize why the correlation linearity may be markedly improved even though the temperature correction is ignored for the LIB signal. For this reason, when the background emission is first normalized by the two-line ratio acquired in 900 ns delay, the correlation plot of Ca LIB/background shows insignificant difference before and after plasma temperature correction at the laser energy 13 mJ (Fig. 10).

D. Characterization of LIB/current correlation

In contrast to the continuum background normalization, when the LIB signal and the corresponding current are correlated, the linearity can be achieved over a much wider range of the laser energy (Fig. 5). The current collected from the droplet ionization is substantially attributed to the electrons, which result mainly from the ionized water–methanol droplets and their fragments.[24] The current response thus obtained is proportional to both the ablated droplet sizes and the electron motion, but irrespective of the sample concentration contained. Increasing the sample concentration may increase the LIB emission intensity, but does not change the current response significantly.[25] The slope in the correlation plot may therefore sensitively reflect the sample concentration. The larger the droplet size ablated, the more the electron amounts (or the current response) are induced. Meanwhile, a higher plasma excitation temperature can speed up the electron motion and then cause a larger current response. The current normalization method seems to have taken into account both the ablated amount of the sample and the plasma excitation temperature.

IV. Conclusion

We have developed a current normalization method for LIBS for analyzing the sample droplets which are generated by an electrospray ionization needle. Upon laser irradiation, the time-resolved LIB profile and the plasma-induced current signal are acquired concurrently. The shot-to-shot correlation plot as a function of the sample concentration yields a calibration curve. The LOD of Na sample thus obtained may reach <1 mg l^{-1}, comparable to those reported previously. In this work, we have characterized both normalization methods of LIB/current and LIB/background as a function of the laser energy. The correlation linearity for the background normalization is restricted within a small range of laser energy, but is significantly improved when a two-line ratio, monitored at the same time as the continuum background, is involved to account for the plasma temperature. A multiple-line method is used to determine the plasma temperature; the temperature gradient is found to be about 1200 ± 1100 K between the 0 and 900 ns delay time when the continuum background and LIB signals are obtained, respectively. Since the temperature fluctuation of the plasma plume is reduced after a 900 ns delay, there is no need to correct the plasma temperature factors simultaneously for both background and LIB signals. In contrast, the correlation linearity with the LIB/current normalization method, which has taken into account the ablated amount of microdroplets and the plasma excitation temperature, may be achieved over a much wider range of laser energy and lead to lower LOD for a sample analysis. This normalization method should be applicable to other LIBS analyses including solid and gas states. In addition, the sampling method with an electrospray ionization device allows one to further couple a flow injection (FI) system. By taking advantage of the *in situ* preconcentration and separation provided by the FI system, the detection sensitivity of LIBS should be enhanced. A related work is in progress.

Acknowledgements

This work is supported by the National Science Council of the Republic of China under Contract No. NSC92-2113-M-001-069.

References

1 M. Capitelli, A. Casavola, G. Colonna and A. De Giacomo, *Spectrochim. Acta, Part B*, 2004, **59**, 271.
2 I. Radivojevic, C. Haisch, R. Niessner, S. Florek, H. Becker-Ross and U. Panne, *Anal. Chem*., 2004, **76**, 1648.
3 V. Bulatov, A. Khalmanov and I. Schechter, *Anal. Bioanal. Chem*., 2003, **375**, 1282.
4 L. J. Radziemski, *Spectrochim. Acta, Part B*, 2002, **57**, 1109.
5 J. E. Carranza and D. W. Hahn, *Anal. Chem*., 2002, **74**, 5450.
6 Y.-I. Lee, K. Song and J. Sneddon in *Lasers in Analytical Atomic Spectroscopy*, eds. J. Sneddon, T. L. Thiem and Y.-I. Lee, VCH, New York, 1997, pp. 197–235.
7 U. Panne, R. E. Neuhauser, C. Haisch, H. Fink and R. Niessner, *Appl. Spectrosc*., 2002, **56**, 375.
8 M. Castillejo, M. Martin, M. Oujja, D. Silva, R. Torres, A. Manousaki, V. Zafiropulos, O. F. van den Brink, R. M. A. Heeren, R. Teule, A. Silva and H. Gouveia, *Anal. Chem*., 2002, **74**, 4662.
9 D. Kossakovski and L. J. Beauchamp, *Anal. Chem*., 2000, **72**, 4731.
10 J. G. Lunney and R. Jordan, *Appl. Surf. Sci*., 1998, **127–129**, 941.
11 S. Amoruso, *Appl. Phys. A*, 1999, **69**, 323.
12 M. Schnurer, R. Nolte, T. Schlegel, M. P. Kalachnikov, P. V. Nickles, P. Ambrosi and W. Sandner, *J. Phys. B*, 1997, **30**, 4653.
13 I. B. Gornushkin, P. E. Eagan, A. B. Novikov, B. W. Smith and J. D. Winefordner, *Appl. Spectrosc*., 2003, **57**, 197.
14 N. H. Cheung and E. S. Yeung, *Appl. Spectrosc*., 1993, **47**, 882.
15 L. Xu, V. Bulatov, V. V. Gridin and I. Schechter, *Anal. Chem*., 1997, **69**, 2103.
16 C. M. Davies, H. H. Telle, D. J. Montgomery and R. E. Corbett, *Spectrochim. Acta, Part B*, 1995, **50**, 1059.
17 C. Aragon, J. A. Aguilera and F. Penalba, *Appl. Spectrosc*., 1999, **53**, 1259.
18 D. A. Cremers, J. E. Barefield and A. C. Koskelo, *Appl. Spectrosc*., 1995, **49**, 857.
19 I. B. Gornushkin, B. W. Smith, G. E. Potts, N. Omenetto and J. D. Winefordner, *Anal. Chem*., 1999, **71**, 5447.
20 J. E. Carranza and D. W. Hahn, *Spectrochim. Acta, Part B*, 2002, **57**, 779.
21 G. Galbacs, I. B. Gornushkin, B. W. Smith and J. D. Winefordner, *Spectrochim. Acta, Part B*, 2001, **56**, 1159.
22 C. Chaleard, P. Mauchien, N. Andre, J. Uebbing, J. L. Lacour and C. Geertsen, *J. Anal. At. Spectrom*., 1997, **12**, 183.
23 H. J. Hakkanen and J. E. I. Korppi-Tommola, *Anal. Chem*., 1998, **70**, 4724.
24 J. S. Huang, C. B. Ke, L. S. Huang and K. C. Lin, *Spectrochim. Acta, Part B*, 2002, **57**, 35.
25 J. S. Huang, C. B. Ke and K. C. Lin, *Spectrochim. Acta, Part B*, 2004, **59**, 321.
26 S. J. Gaskell, *J. Mass Spectrom*., 1997, **32**, 677.
27 J. F. Banks, *Electrophoresis*, 1997, **18**, 2255.
28 A. Gomez and K. Q. Tang, *Phys. Fluids*, 1994, **6**, 404.
29 M. G. Ikonomou, A. T. Blades and P. Kebarle, *Anal. Chem*., 1991, **63**, 1989.
30 Z. Olumee, J. H. Callahan and A. Vertes, *J. Phys. Chem. A*, 1998, **102**, 9154.
31 I. B. Gornushkin, C. L. Stevenson, B. W. Smith, N. Omenetto and J. D. Winefordner, *Spectrochim. Acta, Part B*, 2001, **56**, 1769.
32 A. S. Eppler, D. A. Cremers, D. D. Hickmott, M. J. Ferris and A. C. Koskelo, *Appl. Spectrosc*., 1996, **50**, 1175.
33 G. V. Marr in *Plasma Spectroscopy*, ed. G. V. Marr, Elsevier, New York, 1968, pp. 285–293.
34 S. Yalcin, D. R. Crosley, G. P. Smith and G. W. Faris, *Appl. Phys. B*, 1999, **68**, 121.